

## RESEARCH ARTICLE

# Afadin orients cell division to position the tubule lumen in developing renal tubules

Lei Gao<sup>1</sup>, Zhufeng Yang<sup>1</sup>, Chitkale Hiremath<sup>1</sup>, Susan E. Zimmerman<sup>1</sup>, Blake Long<sup>1</sup>, Paul R. Brakeman<sup>2</sup>, Keith E. Mostov<sup>3</sup>, David M. Bryant<sup>4</sup>, Katherine Luby-Phelps<sup>5</sup> and Denise K. Marciano<sup>1,\*</sup>

## ABSTRACT

In many types of tubules, continuity of the lumen is paramount to tubular function, yet how tubules generate lumen continuity *in vivo* is not known. We recently found that the F-actin-binding protein afadin is required for lumen continuity in developing renal tubules, though its mechanism of action remains unknown. Here, we demonstrate that afadin is required for lumen continuity by orienting the mitotic spindle during cell division. Using an *in vitro* 3D cyst model, we find that afadin localizes to the cell cortex adjacent to the spindle poles and orients the mitotic spindle. In tubules, cell division may be oriented relative to two axes: longitudinal and apical-basal. Unexpectedly, *in vivo* examination of early-stage developing nephron tubules reveals that cell division is not oriented in the longitudinal (or planar-polarized) axis. However, cell division is oriented perpendicular to the apical-basal axis. Absence of afadin *in vivo* leads to misorientation of apical-basal cell division in nephron tubules. Together, these results support a model whereby afadin determines lumen placement by directing apical-basal spindle orientation, resulting in a continuous lumen and normal tubule morphogenesis.

**KEY WORDS:** Kidney development, Lumen, Tubulogenesis, Afadin, Polarity, Nephron, Mouse

## INTRODUCTION

The formation and elongation of epithelial tubules is a central feature of many organs. In the kidney, tubules have a single layer of epithelial cells surrounding a central lumen. Within each tubule, the presence of a continuous lumen is essential to its function: even a small discontinuity would block the passage of filtrate, thereby abolishing its excretory function. Yet how tubules develop a single, continuous lumen with high fidelity is not well understood.

Epithelial tubules are one of the most common tissue types in metazoa, and there is remarkable diversity in the structure and mechanisms by which tubules develop (Marciano, 2017; Iruela-Arispe and Beitel, 2013). Despite differences, a key process in tubulogenesis is the development of cell polarity, the segregation of functionally distinct plasma membrane domains. An epithelial cell

can polarize along its apical-basal axis, which orients the cell relative to the underlying extracellular matrix. The apical surface faces the luminal space, the lateral surface contacts adjacent cells, and the basal surface contacts the basal lamina. Additionally, the individually polarized cells must coordinate their polarity with surrounding cells along the long axis of the tubule, in a process referred to as planar cell polarity.

In the developing kidney, epithelial tubules are derived from progenitor cells from two embryonic sources: the cap mesenchyme and the ureteric epithelium (Saxen, 1987). The cap mesenchyme gives rise to nephron segments from the glomerulus to the distal tubule, and the ureteric epithelium becomes the collecting duct. Whereas the latter arises as a branch from a pre-existing tubule, the cap mesenchyme must undergo a mesenchymal-to-epithelial transition to form a nascent epithelial tubule with *de novo* establishment of apical-basal polarity and generation of a lumen. Study of this process serves as an excellent model to elucidate mechanisms of polarization and tubulogenesis.


In previous studies, we have shown that once a lumen is created, elongation initially occurs by simultaneous extension of the lumen and additional *de novo* lumen generation (Yang et al., 2013). Shortly thereafter, the lumens of developing nephron tubules become continuous, and further elongation of the lumen coincides with elongation of the tubule (Yang et al., 2013).

The cellular mechanisms by which a continuous lumen is generated are poorly understood. *In vitro* studies have demonstrated that formation of a continuous lumen correlates with the axis of cell division (i.e. the orientation of the mitotic spindle) (Jaffe et al., 2008; Hao et al., 2010; Durgan et al., 2011). During mitosis, epithelia orient their mitotic spindle parallel to the apical surface and basal lamina. Defects in this spindle orientation correlate with the formation of multiple lumens *in vitro* (Durgan et al., 2011; Hao et al., 2010; Jaffe et al., 2008). How might this occur? Near the end of cytokinesis, the dividing cell remains interconnected by a bridge-like structure called a midbody. Recent studies have shown that intracellular vesicles carrying apical components localize adjacent to this site, and it has been suggested that the vesicles fuse to this site after abscission to lay down new apical membrane (Klinkert et al., 2016; Schluter et al., 2009; Li et al., 2014). Thus, misorientation of cell division could lead to mispositioning of new apical surface.

To date, the role of oriented cell division in *de novo* lumen formation and continuity during *in vivo* tubulogenesis has not been investigated. However, it has been examined for renal tubule elongation and maintenance, with varying results depending on the type of tubule and stage analyzed (Fischer et al., 2006; Saburi et al., 2008; Sims-Lucas et al., 2012; Nishio et al., 2010; Karner et al., 2009). Interestingly, a study analyzing the elongation of developing renal collecting ducts has shown that spindle orientation is random during development, and only becomes oriented after the neonatal period (Karner et al., 2009). However, as collecting ducts are derived

<sup>1</sup>Department of Medicine, Division of Nephrology, University of Texas Southwestern Medical Center, Dallas, TX, 75390, USA. <sup>2</sup>Department of Pediatrics, University of California, San Francisco, CA, 94158, USA. <sup>3</sup>Department of Anatomy, University of California, San Francisco, CA, 94158, USA. <sup>4</sup>Institute of Cancer Sciences, University of Glasgow and Cancer Research UK Beatson Institute, Glasgow G61 1BD, UK. <sup>5</sup>Department of Cell Biology, University of Texas Southwestern Medical Center.

\*Author for correspondence (denise.marciano@utsouthwestern.edu)

 Z.Y., 0000-0001-6495-2316; C.H., 0000-0003-1770-8112; D.K.M., 0000-0003-0612-4664

from the ureteric epithelia, the mechanisms of tubulogenesis in early nephron tubules from the metanephric mesenchyme, which develop lumen formation *de novo*, remain unknown. Indeed, early-stage nephron tubules have not been examined for oriented cell division, during lumen formation or elongation.

In the current study, we examined mechanisms of lumen continuity by utilizing a mouse mutant that we had previously identified as having defects in lumen formation. Mice lacking the F-actin-binding protein afadin in developing nephron epithelia have both delayed lumen formation and discontinuous lumens (Yang et al., 2013). Afadin is a known component of adherens junctions and tight junctions in fully epithelialized cells, where it is an adaptor to a major class of adhesion receptors called nectins (Mandai et al., 2013). It also is an effector for the small GTPases Rap1 and Rap2 (Boettner et al., 2000; Linnemann et al., 1999; Monteiro et al., 2013), and has been shown to interact with a number of different proteins (Mandai et al., 2013). In addition to its role in cell junctions, afadin orients the mitotic spindle in *Drosophila* neuroblasts (Carmena et al., 2011; Wee et al., 2011) and cortical radial glia (Rakotomamonjy et al., 2017), and has been shown to interact with spindle machinery *in vitro* (Carminati et al., 2016).

To understand how afadin functions to promote a continuous lumen in tubules, we investigated lumen placement *in vitro* in 3D epithelial cell culture and *in vivo* in renal tubules. We show that afadin is required for lumen continuity in a 3D *in vitro* model of renal epithelial lumen formation, demonstrating that it localizes to the cortex overlying mitotic spindles. Lumen discontinuity is dependent on cell division, and afadin orients the mitotic spindle *in vitro*. *In vivo* in developing nephron tubules, a composite measurement of the angle of cell division reveals that cell division is not oriented. This seemingly incongruent result becomes understandable after analysis of the mitotic angle relative to the apical-basal axis. Our analysis demonstrates for the first time that cell division is oriented perpendicular to the apical-basal axis, and this specification of oriented cell division is dependent on afadin. These results support a model in which apical-basal spindle orientation controlled by afadin is necessary to ensure the fidelity of a continuous lumen and normal tubulogenesis.

## RESULTS

### Afadin is required for timely lumen initiation and continuity *in vivo* and *in vitro*

During nephrogenesis, nephron progenitors from the cap mesenchyme condense to form a pretubular aggregate, and then undergo epithelialization to form a spherical structure with a central lumen called the renal vesicle. The renal vesicle then undergoes proliferation and morphogenesis to form an s-shaped tubule aptly called the s-shaped body. We have previously shown that afadin is required for normal lumen formation in developing nephrons (Yang et al., 2013). Mice with conditional deletion of afadin using the *Pax3-cre* transgenic line display both a delay in the onset of lumen initiation and then develop discontinuous lumens in developing nephrons (Yang et al., 2013). Deletion of the afadin gene (*Afdn*) specifically within nephron progenitors (*Afdn*<sup>fl/fl</sup>; *Six2-cre*) causes similar defects, with mutant mice ultimately developing severe renal dysplasia and dying at 4–6 weeks of age (Yang et al., 2013). Fig. 1 shows that s-shaped bodies from *Afdn*<sup>fl/fl</sup>; *Six2-cre* mice had numerous discontinuous lumens compared with control littermates (Fig. 1A–C, Fig. S1). The lumens were demarcated by Par6 (Pard6b) at the apical surface and ZO1 at apical junctions (Fig. 1B). Some of the later-stage, more elongated nephron tubules also had abnormal morphogenesis and more than one lumen transversely, appearing multi-layered (Fig. 1C).

To ensure that the discontinuous lumen phenotype was not secondary to the delay in lumen creation, we also examined mice with conditional deletion of *Afdn* using *Wnt4-cre*, which results in *Cre*-mediated recombination at the pretubular aggregate/renal vesicle stage. In these mutant mice, afadin was still present in renal vesicles and variably decreased in s-shaped bodies (Fig. S2A). These mutant kidneys had lumens of normal appearance in renal vesicles [27 of 27 renal vesicles from two *Afdn*<sup>fl/fl</sup>; *Wnt-cre* postnatal day (P) 0 mice], but 30% of s-shaped bodies had discontinuous lumens (9 of 27 s-shaped bodies from two *Afdn*<sup>fl/fl</sup>; *Wnt-cre* P0 mice) (Fig. S2B). The reduced penetrance of lumen discontinuities in *Afdn*<sup>fl/fl</sup>; *Wnt-cre* mice compared with *Afdn*<sup>fl/fl</sup>; *Six2-cre* mice is likely to be due to residual afadin in the former. These results indicate that the delay in lumen initiation and the lumen discontinuity represent two distinct phenotypes.

To determine whether afadin played a similar role in the ureteric epithelial tubules, we conditionally deleted *Afdn* using the *HoxB7-cre* line. As described earlier, these tubules arise by branching/budding from a pre-existing tubule, and their lumens form by extension of a pre-existing lumen, not *de novo*. We examined 22 3D reconstructions of ureteric tubules from three *Afdn*<sup>fl/fl</sup>; *HoxB7-cre* neonatal mice, and all had fully continuous lumens (Fig. S3A). However, residual afadin was observed by immunostaining in nearly half of all ureteric tubules (48%, 13 of 27 from two *Afdn*<sup>fl/fl</sup>; *HoxB7-cre* mutants) (Fig. S3B). Because half of the ureteric tubules did not appear to have afadin, it is reasonable to conclude that afadin does not have a major role in lumen continuity of ureteric epithelia.

To elucidate the mechanism by which afadin regulates lumen formation, we utilized a well-established 3D model of renal epithelial lumen formation employing Madin–Darby canine kidney (MDCK) cells (Marciano et al., 2011; O'Brien et al., 2001). When individual MDCK cells are cultured in a 3D gel of extracellular matrix, they proliferate and form fluid-filled spheres called cysts that are lined by a monolayer of polarized cells. Lumen formation can be studied at discrete stages that are marked, in part, by the localization of podocalyxin (Podxl1; Podxl) (Fig. 2A). Podxl1 is initially peripheral (Fig. 2Aa), and then is internalized to form intracellular vesicles (Fig. 2Ab, arrows). These vesicles fuse at the cell-cell junction, forming the apical membrane initiation site (AMIS) (Fig. 2Ac), which expands to become what is referred to as a pre-apical patch (PAP) (Fig. 2Ad), and ultimately forms an open lumen (not shown). This lumen expands as the size of the cysts increases (Fig. 2Ae). Using these stages, we found that afadin underwent a dynamic relocalization during lumen formation. Afadin was first localized to the cell-cell interface and was excluded from the AMIS (Fig. 2Ac). It remained excluded from the PAP and became restricted to apical cell junctions (Fig. 2Ad).

To determine the role of afadin in lumen formation, we generated MDCK cells stably depleted of afadin using shRNA. Afadin knockdown (Af KD) cysts were devoid of afadin by immunostaining (Fig. 2B, compare arrows in control and Af KD) and western blot (Fig. 2C). To control for off-target effects, we generated afadin knockout (Af KO) cell lines using gene editing (Fig. 2B,C). Afadin KD and KO showed similar phenotypes, as described below.

We first wanted to assess the role of afadin in the timing of lumen initiation using the MDCK cyst assay. Although we had previously shown that mice with conditional deletion of *Afdn* using *Pax3-cre* have a significant delay in lumen initiation (Yang et al., 2013), this phenotype could have arisen from several factors, including a delay in the mesenchymal-to-epithelial transition, differentiation, or



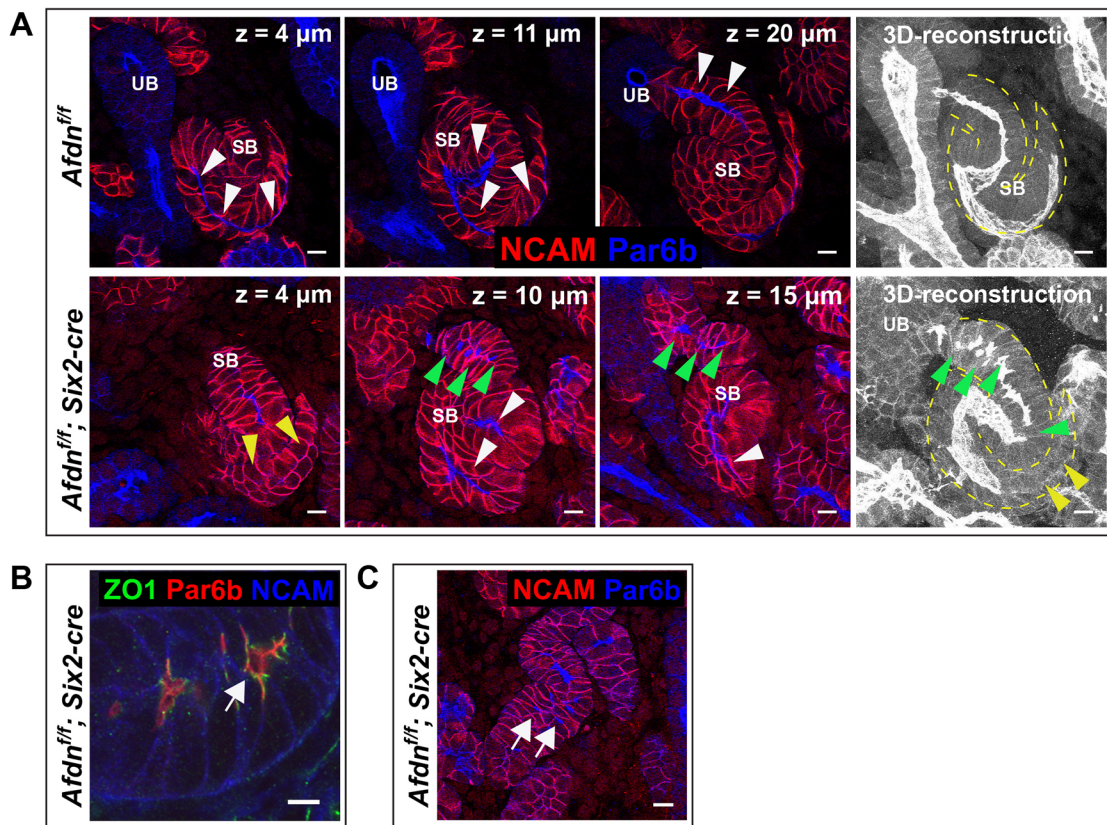


**Fig. 1. Absence of afadin from renal tubules causes discontinuous lumens.** (A) Selected confocal images of z-stacks from early-stage nephron tubules called s-shaped bodies in control (*Afdn<sup>fl/fl</sup>*) and mutant (*Afdn<sup>fl/fl</sup>; Six2-cre*) mouse kidney at E17.5. Immunofluorescence depicts a basolateral marker (NCAM, red) and an apical marker (Par6b, blue). The z-plane is indicated. Arrowheads show the expected location of the tubular lumens, with white indicating a normal lumen segment, yellow indicating an absent lumen and green indicating a discontinuous lumen. A 3D reconstruction of the s-shaped body (right, outlined with a yellow dashed line) shows a continuous lumen in the control, whereas the mutant lumen is partially absent and shows numerous discontinuities. Results are representative of  $n=4$  embryos for each genotype. SB, s-shaped body; UB, ureteric bud. (B) Confocal image of an afadin mutant at E17.5 immunostained with ZO1 (a marker of tight junctions), Par6b and NCAM. A small lumen (arrow) is delineated by ZO1. (C) Confocal image of an afadin mutant at E17.5 as in A showing a slightly later, more elongated, tubule. Arrows indicate multiple lumens that appear to be layered. Scale bars: 10  $\mu$ m (A,C); 4  $\mu$ m (B).

lumen initiation. To study the process *in vitro*, we quantified the early stages (20 h) of lumen formation in two-cell cysts with and without afadin (Fig. 2D). This analysis revealed that among the early-stage afadin KO cysts there were fewer cysts with a single lumen at 20 h. The afadin KO cyst group had more cysts at the AMIS stage, suggesting that afadin is required for timely initiation of the PAP stage. The results demonstrate that afadin is required for timely lumen initiation *in vitro*.

In addition to a delay in lumen initiation, the most pronounced phenotype we observed was a multi-lumen phenotype at later time points (Fig. 2E,F), similar to the murine *in vivo* phenotype (Fig. 1). Indeed, it is this phenotype that will be the focus of the rest of the paper. Many of the 5-day cysts lacking afadin contained several lumens, as illustrated in Fig. 2E. We did note, however, that there was no obvious loss in polarity per se. The basolateral marker cadherin 6 and apical marker podocalyxin seemed to have normal localization compared with controls in 5-day cysts, and in two-cell cysts that had already formed a lumen (Fig. 2E). Similarly, ZO1, a marker of tight junctions, appeared to be correctly localized.

#### Lumen continuity is a dynamic process affected by lumen coalescence and cell division

The total number of lumens within a cyst reflects a balance between the creation of new lumens and fusion of existing lumens. We found

that at an early time point (2 days), nearly 50% of control cysts had developed multiple lumens (Fig. 3A). This percentage decreased over time (Fig. 3A), suggesting that lumen fusion predominates over the generation of new lumens in normal cysts, consistent with prior reports (Cerruti et al., 2013). To examine this process in cysts lacking afadin, we quantified the number of lumens in control and Af KO cysts at 2 days and 4 days (Fig. 3B). Consistent with our time course data, at 4 days, control cysts had an increase in single-lumen cysts (Fig. 3B) and a decrease in the number of lumens per cyst (Fig. 3C) compared with those at 2 days. However, in Af KO cysts there was both a small increase in the single lumen cysts and an increase in the number of cysts with >4 lumens (Fig. 3B, compare Af KO at day 2 with Af KO at day 4), such that the average total number of lumens per cyst was unchanged (Fig. 3C). Because there was an increase in the percentage of cysts with >4 lumens, this suggested that the multi-lumen phenotype may be, at least in part, due to the creation of new lumens.

We next sought to determine the cellular mechanisms that contribute to creation of excessive new lumens in Af KO cysts. Recent data has shown that cell division is coupled with lumen formation and lumen position (Bañón-Rodríguez et al., 2014; Jaffe et al., 2008). We examined whether afadin controls lumen number via a role in cell division. We blocked/inhibited cell division with thymidine treatment, which has previously been shown to slow cell division (Bañón-Rodríguez et al., 2014), in control and Af KO cysts

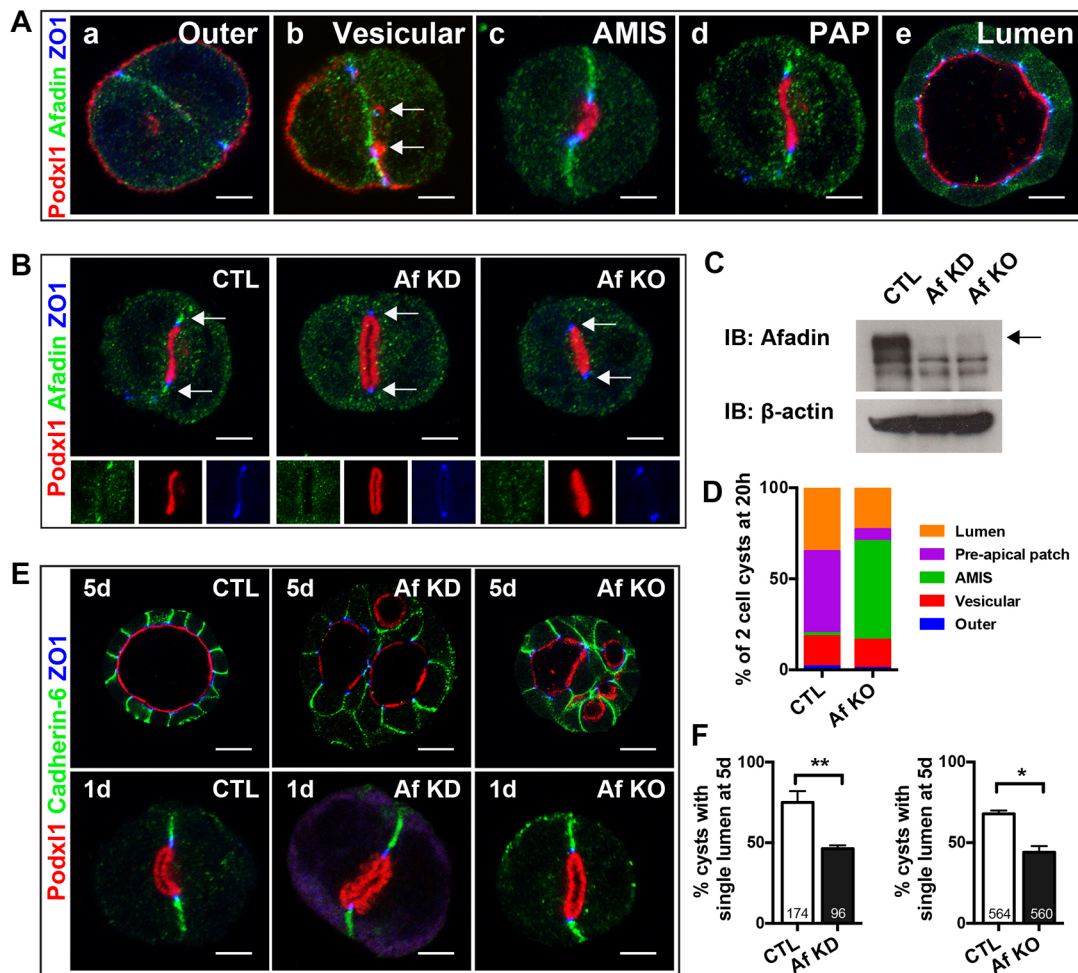


**Fig. 2. Afadin is required for timely lumen initiation and single lumen formation in MDCK cysts.** (A) Afadin localization during cyst formation. (a) At the two-cell stage, afadin localizes to the cell-cell interface, ZO1 localizes to the lateral cell interface, and Podxl1 localizes to the outer periphery. (b) Podxl1 is internalized into vesicles (arrows) and transcytosed during lumen initiation to a site containing ZO1 but not afadin. (c) Afadin is absent from apical membrane initiation site (AMIS), but present at apical cell junctions (where it colocalizes with ZO1) and at the cell-cell interface. Afadin becomes restricted to apical cell junctions at the pre-apical patch (PAP) stage (d) and the open lumen stage (not shown), including later cysts, such as the 5-day cyst (e). At the apical cell junction, afadin partially colocalizes with ZO1, but some is basal to ZO1. (B,C) Immunofluorescence of afadin in 1-day cysts (B) and western blot of afadin in 5-day cysts (C) with shRNA-mediated afadin knockdown (KD) and CRISPR-Cas9-mediated afadin knockout (KO). (D) Quantification of the percentage of cysts at the indicated pre-luminal stages at 20 h. See text for details. (E) Immunofluorescence of Podxl1, cadherin 6, and ZO1 in 1-day and 5-day cysts with afadin KD and KO showing localization of these proteins. Cysts lacking afadin (KD and KO) have multiple lumens at day 5. (F) Quantification of the percentage of cysts with a single lumen at 5 days. Data are mean $\pm$ s.d. There is a significant reduction in cysts with a single lumen in afadin KD (\*\* $P$ <0.002) and KO (\* $P$ <0.02) cysts. Results are representative of at least two independent experiments. Numbers at base of bars indicate the number of cysts analyzed. Scale bars: 5  $\mu$ m (Aa–Ad, B, E upper panels); 10  $\mu$ m (Ae, E lower panels).

at 2 days. We added thymidine to 2-day cysts rather than 1-day cysts because 1-day cysts had few cells and generally zero or one lumen. The addition of thymidine caused a 15% decrease in the total number of lumens per cyst in Af KO cysts ( $P$ ≤0.01) (Fig. 3C). Although this was a consistent but modest reduction, it suggested that the excessive number of lumens formed in the absence of afadin is linked to cell division, and led us to the next set of experiments.

#### Afadin orients the mitotic spindle in cultured renal epithelial cells

Misorientation of the mitotic spindle has been associated with a multi-lumen phenotype (Durgan et al., 2011; Hao et al., 2010; Jaffe et al., 2008), which is thought to be due to mispositioning of the newly generated apical surface that occurs after cell division. To determine whether afadin contributes to the orientation of the mitotic spindle in renal epithelia, we first examined afadin localization during mitosis in early MDCK cysts. Afadin

localized to the lateral cell cortex adjacent to the spindle poles, marked by  $\alpha$ -tubulin, during metaphase and anaphase (Fig. 4Aa–Ac, compare with 4Ad–Af). Afadin also localized to the area surrounding the midbody during cytokinesis (Fig. S4).

We examined the orientation of cell division relative to the apical-basal axis in control and Af KO cysts at 5 days in both metaphase and anaphase. Anaphase was examined to limit errors because the spindle rotates in prometaphase (Reinsch and Karsenti, 1994). The spindle angle was measured relative to a radial vector (defined as the apical-basal axis) from the center of the cysts. The Af KO cysts had misorientation of mitotic spindles in both metaphase and anaphase (Fig. 4B,C). Because many of the Af KO cysts at 5 days had multiple, misplaced lumens, we also considered that the lumen itself could potentially act as a cue for spindle orientation, with misplaced lumens redirecting spindle orientation. Thus, we quantified the orientation of cell division in early-stage cysts (20 h) that contained zero or one lumen (Fig. 4D). These results



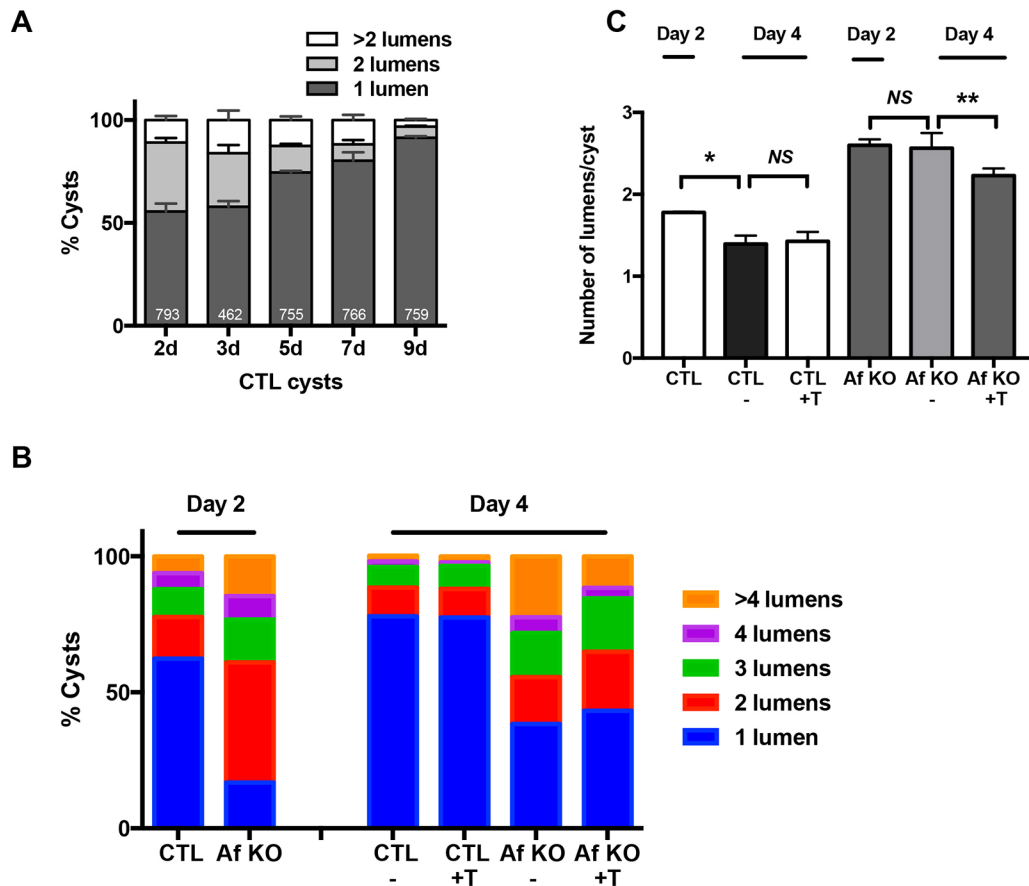


**Fig. 3. Fusion of lumens occurs to generate single lumen cysts.** (A) Quantification of the percentage of multi-lumen cysts over time in control cysts. Numbers at base of bars indicate the number of cysts analyzed. (B) Quantification of lumen number in cysts from controls or afadin KO cysts treated  $\pm$ thymidine (T) at 48 h and harvested at 96 h (4 days). (C) Data from B is shown as the total number of lumens/cyst at day 2 and day 4. Data was analyzed with a one-way ANOVA and Sidak's multiple comparisons test was used to adjust *P*-values for multiple comparisons. Control cysts have fewer lumens at 4 days compared with 2 days ( $*P < 0.004$ ), but afadin KO cysts do not. Afadin KO cysts treated with thymidine at 2 days have a reduction in lumens compared with untreated cysts at 4 days ( $**P \leq 0.01$ ). Results in A-C are representative of at least two similar experiments. NS, not significant.

showed that AfKO cysts had loss of spindle orientation very early in cyst formation. This suggested that the defect in orientation of cell division is primary, occurring prior to the formation of multiple lumens. Thus, we concluded that afadin regulates the apical-basal orientation of cell division *in vitro* in renal epithelial cells.

Because the absence of afadin caused a spindle orientation defect, its role in midbody placement, which forms during late cytokinesis, could not be independently assessed in 3D models (or *in vivo*). It is worth noting that the absence of afadin did not lead to multinucleated cells (not shown), demonstrating that it does not have an essential role in cytokinetic abscission.

#### Developing renal tubules orient the apical-basal component of the mitotic spindle angle in an afadin-dependent manner

Because disruption of spindle angle (as a result of loss of afadin) correlated with multiple lumens *in vitro*, and absence of afadin caused multiple, discontinuous lumens *in vivo*, we decided to examine orientation of cell division in developing nephron tubules. We first imaged transverse sections in 2D from developing control nephrons. We examined mitotic cells in anaphase in a late renal vesicle (Fig. 5A,A') and developing tubule (Fig. 5B,B') and observed that the orientation of division appeared to be parallel to the luminal/apical surface, i.e. perpendicular to the apical-basal axis of the epithelium. This is consistent with our observations in MDCK

cysts (see Fig. 4B). We also observed that the midbody, the transient structure that is formed near completion of cytokinesis, is placed apically in developing nephrons (Fig. 5C,C'). This also is consistent with *in vitro* data that have demonstrated that cytokinesis occurs asymmetrically in epithelia (Reinsch and Karsenti, 1994; Morais-de-Sá and Sunkel, 2013), and suggests that cell division occurs perpendicular to the apical-basal axis.

Within tubules, oriented cell division occurs when the mitotic spindle (and nuclear chromatid) vector is parallel to the longitudinal axis and perpendicular to the apical-basal axis of the tubule (Fig. 6A, a). Defects in either longitudinal (Fig. 6A, b) and/or apical-basal orientation (Fig. 6A, c) lead to misoriented cell division. Mitotic spindle orientation in dividing renal epithelial cells can be determined by measuring the angle ( $\theta$ ) between the vector comprising the long axis of the tubule (the reference vector) and the vector of the mitotic spindle/chromatids, shown schematically in Fig. 6B. Additionally, to assess its apical-basal orientation specifically, one can also measure a projected angle relative to the apical-basal axis of the epithelium ( $\phi$ ), as shown in Fig. 6C (Tang et al., 2011). To measure these angles, we generated 3D reconstructions of *z*-stacks from immunostained developing nephrons. We analyzed NCAM-positive tubules, which included s-shaped bodies and slightly more mature tubules. Measurements of earlier stages were not possible owing to difficulties in determining the reference vector.

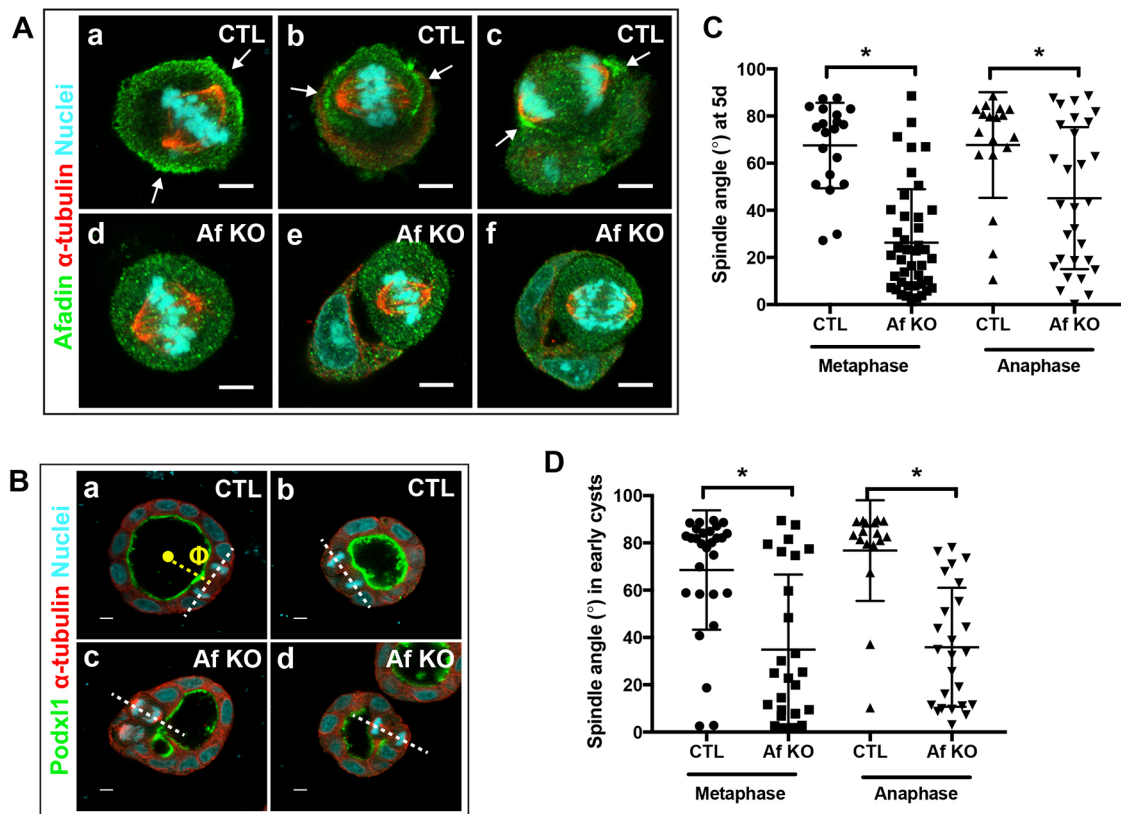


**Fig. 4. Afadin orients the mitotic spindle.** (A) Confocal images of immunofluorescence of afadin (green) and  $\alpha$ -tubulin (red), a marker of the spindle, during metaphase at the one- to two-cell stage (a,d), metaphase at the two- to three-cell stage (b,e), and anaphase (c,f) in control and afadin KO MDCK cysts. (B) Confocal images of 5-day MDCK cysts immunolabeled with Podxl1,  $\alpha$ -tubulin and nuclei show representative spindle orientation. White dashed lines indicate the spindle vectors. A schematic of how the spindle angle was measured is shown in Ba (yellow). (C) Quantification of spindle angles relative to the apical-basal axis in metaphase and anaphase from 5-day cysts ( $*P<0.002$ ). (D) Quantification of spindle angles in early-stage cysts (24 h) as in panel A ( $*$  and  $**P<0.0001$ ). Results are representative of at least two independent experiments. Scale bars: 5  $\mu$ m.

A representative z-stack of a control tubule (Fig. 6D) shows that although chromatid/spindle vectors do not appear to be oriented parallel to the long axis of the tubule (Fig. 6Db,Dc), the  $\phi$  angles are oriented at almost  $90^\circ$  relative to the apical-basal axis (Fig. 6Db1,Dc1).

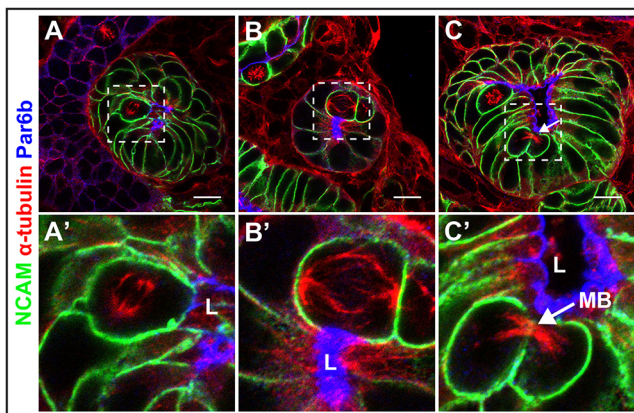


**Fig. 5. Spindle angle and midbody placement in developing renal vesicles.** (A-C') Immunolabeling of microtubules with  $\alpha$ -tubulin (red) shows the mitotic spindle (A,B) and the midbody (C), which contains concentrated microtubules, in developing nephron tubules. The apical surface is marked by Par6b (blue) and the lumen (L) is indicated. Spindles appear parallel to basal and apical surfaces in a renal vesicle (A) and later tubule (B). Midbodies are apically located (C, arrow). A'-C' are high magnifications of the boxed areas in A-C. Scale bars: 10  $\mu$ m.

It also illustrates that dividing cells 'round up' and move near the center of the tubule (Fig. 6Db1,Dc1), as has been demonstrated in epithelial cultures (Reinsch and Karsenti, 1994) and in elegant imaging studies of developing ureteric epithelium (Packard et al., 2013).

Using our 3D reconstructions, we measured the orientation of cell division using the angle  $\theta$  and the apical-basal angle  $\phi$  (Fig. 6E,F). In control nephron tubules,  $\theta$  appeared to be uniformly distributed ( $P=0.34$ , D'Agostino and Pearson normality test). This result in developing nephrons is similar to previously published results for developing collecting ducts, which also do not have oriented cell division (Kamer et al., 2009). Our measurements of  $\phi$  added additional information, showing that the orientation of cell division in the apical-basal axis was not uniformly distributed ( $P<0.001$ , D'Agostino and Pearson normality test), but skewed toward higher angles (skewness =  $-1.6$ ). Thus, the apical-basal component of cell division is oriented.

We next examined the role of afadin in oriented cell division *in vivo*. In *Afdn<sup>fl/fl</sup>; Six2-cre* tubules, analysis of  $\theta$  showed that spindle orientation distribution across the entire angular range was not different from control tubules. However, there was a difference in  $\phi$  between controls and mutant tubules (mean $\pm$ s.d.:  $77\pm 8$  and  $57\pm 23$ ,  $P<0.001$ ) (Fig. 6E), with mutants having a more uniform distribution of  $\phi$ . Whereas control tubules had no mitoses with  $\phi<50^\circ$ , 35% of mutant tubules had  $\phi<50^\circ$  (Fig. 6F). Together, our data demonstrate *in vivo* the importance of afadin in regulating apical-basal orientation of cell division and continuous lumen formation.



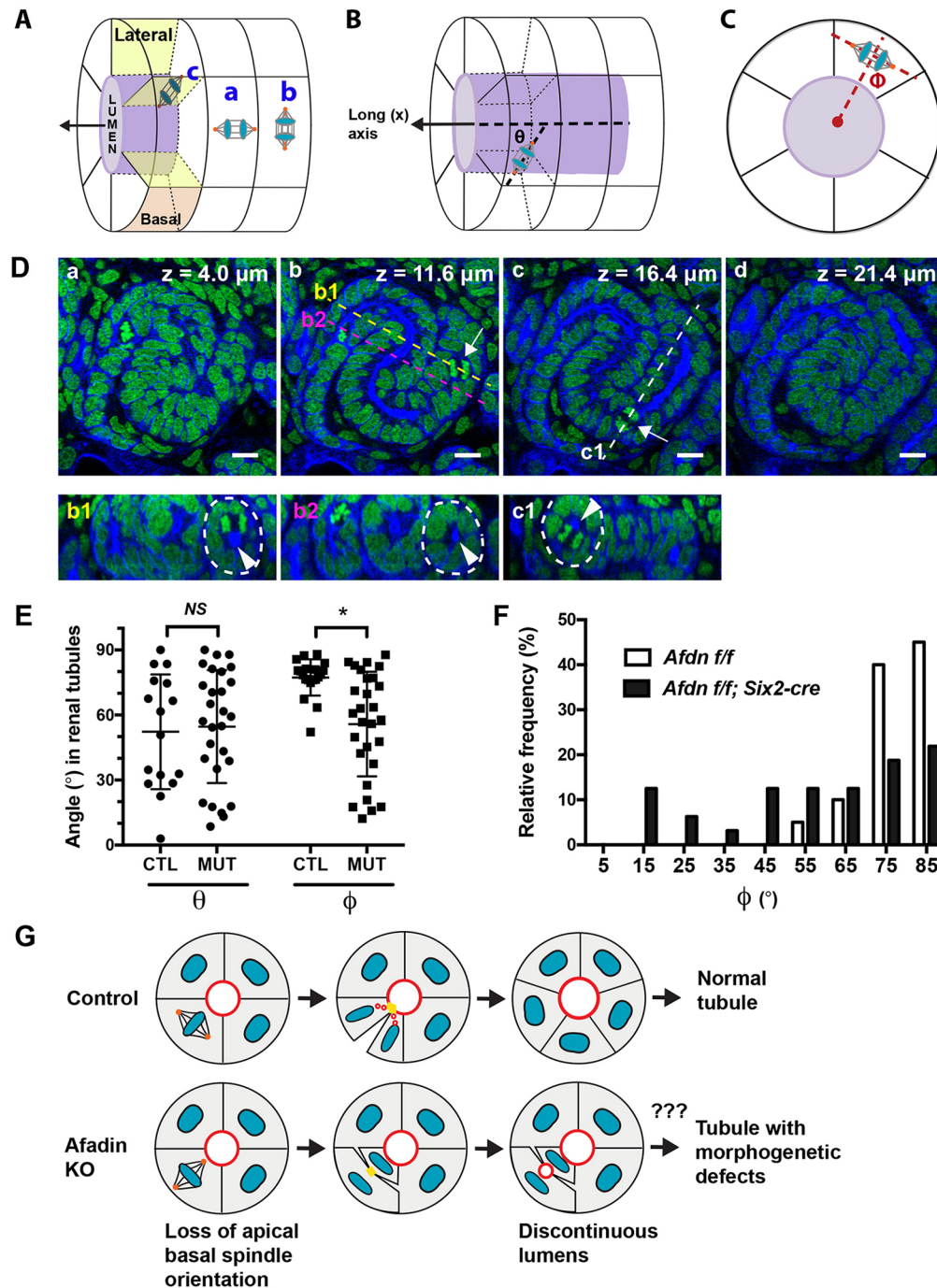


**Fig. 6. Afadin is required for spindle orientation in developing nephron tubules.** (A) Schematic showing orientation of cell division. Oriented cell division occurs when the mitotic spindle is parallel to the longitudinal axis and perpendicular to the apical-basal axis of the tubule (a). Misorientation of cell division occurs with defects in the longitudinal (b) and/or apical-basal orientation (c) of cell division. (B,C) Diagrams representing how the orientation of cell division was determined within a nephron tubule. Angle  $\theta$  is the angle between the longitudinal axis of the tubule and the spindle vector. Angle  $\phi$  is the apical-basal component of the spindle angle measured as the angle between the spindle/chromatid vector and a radial vector, as seen in a transverse section of the tubule. For example, a measurement of  $\phi = 90^\circ$  indicates that the cell is dividing perpendicular to the apical-basal axis and is correctly oriented. (D) Selected images of a z-stack of a control s-shaped body/tubule. F-actin (blue) and nuclei (green) are shown. z-axis depth is indicated and two mitotic cells in anaphase are shown (arrows in Db and Dc). The mitotic axes of the dividing cells in Db, and perhaps Dc, do not appear to be oriented along the longitudinal axis; however, transverse sections at b1 and c1 shows they are oriented nearly parallel to the apical and basal surfaces. Db1 also shows the dividing cell (and its chromatids) have moved into the lumen of the tubule (arrowhead) relative to other cells, whose nuclei are basal. The position of nuclei in non-dividing cells of an adjacent transverse section is shown for comparison. Scale bars: 10  $\mu\text{m}$ . (E) Analysis of  $\theta$  and  $\phi$  mitotic angles in control (*Afdn<sup>fl/fl</sup>*) and mutant (*Afdn<sup>fl/fl</sup>; Six2-cre*) kidneys at E17.5 ( $n = 3$  for each genotype). In controls,  $\theta$  is uniformly distributed, but  $\phi$  is skewed toward higher angles (see text). The  $\phi$  angles are different in controls and mutants (\* $P < 0.001$ ). NS, not significant. (F) Histogram analysis of  $\phi$  in E. (G) Model of the role of afadin in lumen continuity and tubulogenesis. In control tubules, afadin regulates spindle orientation, thus allowing correct lumen placement and normal tubulogenesis. Without afadin, apical-basal spindle orientation is disrupted, leading to misplacement of lumens. We speculate that lumen misplacement leads to morphogenetic defects in the tubules.

## DISCUSSION

Lumen continuity is essential to renal tubule function, but our knowledge of the mechanisms that promote its formation is limited. In addition, the role of oriented cell division in generating a continuous lumen *in vivo* is unknown, although it has been studied in other contexts (Fischer et al., 2006; Saburi et al., 2008; Sims-Lucas et al., 2012; Nishio et al., 2010; Karner et al., 2009). In this study, we sought to identify cellular mechanisms that regulate the generation of a continuous lumen *in vivo* in renal tubules. We demonstrate that afadin determines lumen continuity and directs spindle orientation, which we find to be highly oriented perpendicular to the apical-basal axis.

We initially utilized a 3D cyst model in which the absence of afadin *in vitro* recapitulates the phenotype of multiple discontinuous lumens previously described in developing renal tubules. Specifically, there is a delay in lumen formation, and then multiple, discontinuous lumens are generated when afadin is deleted from MDCK cell cysts. We found that once the initial lumen is generated, the cysts have a clear demarcation of apical and basal plasma membranes, despite their multiple lumens, suggesting that afadin is required to position the apical surface.

The 3D *in vitro* studies of lumen generation suggest that both luminal fusion and creation of new lumens contribute to final lumen number. During early cystogenesis, nearly half of all cysts have more than one lumen, generally two, but this proportion dramatically decreases over time. This suggests that fusion to a single lumen predominates over the generation of new lumens in control cysts.

In contrast, cysts lacking afadin have a high number of lumens during early cystogenesis, which do not decrease over time, at least initially (from day 2 to day 4). Although the percentage of afadin-depleted cysts with a single lumen increases over time, this is offset by increased lumen number in the remaining cysts. Together, these data suggest that luminal fusion is not blocked in the absence of afadin, and that additional new lumens are generated.

There is growing evidence in the literature that cell division plays an important role in the creation of new apical/luminal surfaces. Indeed, our *in vitro* experiments show that inhibition/slowing of cell division decreased the number of lumens in cysts lacking afadin. Studies of the first mitotic event in MDCK cysts have demonstrated that during cytokinesis, vesicles carrying apical membrane components localize in close proximity to the cytotkinetic bridge microtubules and then fuse to the apical membrane initiation site at the cell-cell interface between the newly divided cells (Klinkert et al., 2016; Schluter et al., 2009; Li et al., 2014). After the initial lumen is formed, in subsequent mitotic events, the axis of cell division (i.e. the orientation of the mitotic spindle) is oriented parallel to the basal lamina and apical surface *in vitro*. Both polarity proteins and the spindle machinery direct spindle orientation (Schober et al., 1999; Wodarz et al., 1999; Hao et al., 2010), and loss of one of these proteins leads to both misoriented spindles and multiple lumens. This suggests that the axis of cell division is important for maintaining the position of the apical surface, thus allowing for further extension of a single lumen after cell division.

It is important to note that although cell division is generally oriented in MDCK cysts, as mentioned previously, many cysts initially develop more than one, generally two, lumens. However, corrective mechanisms, e.g. luminal fusion, exist to return the cyst to a single lumen state. It is likely that the defects in the afadin-depleted cysts overwhelm the capacity of these corrective mechanisms.

In contrast to *in vitro* studies, examination of oriented cell division in renal tubules has led to differing results (Fischer et al.,

2006; Saburi et al., 2008; Sims-Lucas et al., 2012; Nishio et al., 2010; Karner et al., 2009). These discrepancies might be due to differences in tubule stage (early and late developmental stages, and mature tubules), location (cortical versus medullary), and type of tubule. Our own studies of developing nephron tubules found that overall cell division is not oriented, as measured by the angle ( $\theta$ ) between the long axis of the tubule and the spindle vector. Similar results have been obtained in developing ureteric epithelial tubules (Karner et al., 2009), suggesting that random orientation of  $\theta$  during embryogenesis might be a general feature of renal epithelia. Our result also initially suggested correct spindle orientation is not required for lumen continuity (or tubule morphogenesis), which implied that other factors, such as cellular movements, might be responsible for generating tubules with a continuous central lumen. However, spindles can be oriented by planar polarity and apical-basal polarity, and measurement of  $\theta$  encompasses both. Because only defects in apical-basal polarity would be expected to cause lumen discontinuity, we performed additional analysis to measure the apical-basal projection angle ( $\phi$ ). Measurement of  $\phi$  showed that cell division is consistently oriented nearly perpendicular to the apical-basal axis, indicating that spindles are indeed oriented by apical-basal polarity in embryonic tubules. Consistent with this, we found that midbody placement in these tubules is apical, as has been reported for *in vitro* epithelia (Morais-de-Sá and Sunkel, 2013). Thus, in nephron tubules, although overall cell division is not oriented, the component corresponding to apical-basal polarity is oriented.

Our results also demonstrate that afadin mutants have disrupted apical-basal orientation of cell division and discontinuous lumens in developing nephron epithelial tubules and in *in vitro* cysts. Thus, defects in the apical-basal orientation of cell division could contribute to the luminal defects in afadin mutants. Because spindle angles are generally measured relative to the basal, not apical, surface of a tubule or cyst, we considered that perhaps the multiple, ectopic apical surfaces/lumens in afadin mutants were acting as ‘orienting cues’, which would make spindles appear misoriented with respect to the basal surface. However, examination of early 3D cysts showed that those lacking afadin have spindle misorientation even prior to the multiple lumen phenotype.

Although this study was conducted to examine regulation of lumen continuity and placement, it is difficult to fully separate lumen continuity from tubule elongation/morphogenesis, as these processes are likely to be interrelated. Some late-stage nephron tubules lacking afadin have morphogenetic defects, indicating that lumen placement correlates with morphogenesis. However, in afadin mutant mice, defects in lumen continuity precede morphogenetic defects. Additionally, afadin KO cysts have abnormal lumen placement with normal spherical structure, indicating that a morphogenetic defect does not cause the defect in lumen placement and spindle orientation *in vitro*. Thus, abnormal lumen placement in the absence of afadin is likely to be the primary defect. Our results are most consistent with a model in which absence of afadin results in loss of apical-basal spindle orientation, which leads to multiple, misplaced lumens, contributing to morphogenetic defects, as shown schematically in Fig. 6G.

Together, our results support a model in which afadin positions the placement of newly generated apical/luminal plasma membrane at least in part through its role in spindle orientation, leading to lumen continuity. This novel finding for the role of afadin requires further mechanistic study and is the focus of our ongoing work. Additionally, although our analysis has focused on the role of spindle orientation and apical-basal positioning of the lumen, afadin



has a well-known role in adherens junction formation and has also been implicated in directional cell migration (Mandai et al., 2013; Sawyer et al., 2011). Both of these processes could also affect lumen continuity and/or tubule morphogenesis *in vivo*. Indeed, cell movements have been shown to resolve lumen discontinuities in *in vitro* epithelial tubes (Kim et al., 2015). Future studies, particularly those using live imaging, will be needed to elucidate the roles of these various processes in tubulogenesis.

## MATERIALS AND METHODS

### Animals and histology

We crossed conditional *Afdn* (*Afdn<sup>fl/fl</sup>*) females to *Afdn<sup>fl/+</sup>; Six2-cre<sup>Tg</sup>* (Kobayashi et al., 2008) males to obtain *Afdn<sup>fl/+</sup>; Six2-cre* mutant mouse embryos. Mice with conditional deletion of afadin with *Wnt4-cre* (Mugford et al., 2009) and *HoxB7-cre* (Yu et al., 2002) were also generated. Mice were maintained on mixed genetic backgrounds and genotyped by standard PCR. Embryonic day (E) 17.5 kidneys of both sexes were harvested and fixed for 2 h in 4% paraformaldehyde in PBS. Procedures were performed according to UTSW-IACUC-approved guidelines.

### MDCK culture, shRNA-mediated gene silencing and CRISPR gene editing

MDCK type II cells were grown and imaged as described previously (Marciano et al., 2011; Mostov and Deitcher, 1986) and tested for mycoplasma contamination. Afadin shRNA was based on published shRNA from Y. Takai (Sato et al., 2006) and is shown in Table S1. For the control, we utilized a scramble shRNA, as we have done previously (Marciano et al., 2011). shRNAs were cloned into pLKO.1 puromycin. Viral transduction of MDCK cells was performed as previously described (Bryant et al., 2010).

For CRISPR knockout lines, sgRNA oligonucleotides were designed using the CRISPR Genome Engineering Resources (<http://crispr.mit.edu/>). Knockout (KO) clones were generated and selected according to a published protocol (Cong and Zhang, 2015). Clones were verified for loss of afadin using western blot. The sgRNAs used to generate clones for this study are included in Table S1.

For cysts treated with thymidine, we first performed a dosage curve to establish the concentration of thymidine that would inhibit MDCK cell proliferation but not result in cell death by 48 h (data not shown). We added this dose (2  $\mu$ M thymidine) to cysts at 48 h, and analyzed the effect on lumen number 48 h later.

### Immunofluorescence

Immunostaining was performed as previously reported (Yang et al., 2013). Briefly, kidney sections were permeabilized with 0.3% Triton X-100/PBS (PBST) and blocked with 10% donkey sera/PBST. For cells, samples were permeabilized with 0.3% PBST and blocked with 0.7% fish skin gelatin in TBS with 0.025% saponin (TFS). Samples were incubated with primary antibodies overnight (4°C), then with fluorophore-conjugated secondary antibodies. Kidney sections were mounted with Prolong Gold (Invitrogen). Confocal imaging was performed on a Zeiss LSM510 META laser scanning confocal microscope. Images were analyzed using ImageJ software. Images were minimally processed and re-sampled to 300 dpi using Adobe Photoshop.

### Western blot

MDCK cysts were lysed in ice-cold buffer containing 1% Triton X-100, 0.5% sodium deoxycholate, 0.1% SDS, 20 mM sodium phosphate (pH 7.2), 150 mM NaCl, 50 mM Tris-HCl, 1 mM NaF, 1 mM Na<sub>3</sub>VO<sub>4</sub>, 1 mM PMSF and a protease inhibitor cocktail (Roche). Lysates were centrifuged at 17,000 g for 15 min at 4°C to remove insoluble aggregates, and SDS-PAGE and western blotting were performed.

### Antibodies

For kidney immunostaining, primary antibodies were used at 1:100 unless stated otherwise: afadin (Sigma, A0224), NCAM [Developmental Studies

Hybridoma Bank (DSHB), 5B8; GeneTex, H28-123],  $\alpha$ -tubulin (AbD Serotec, MCA77G), Par6b (SCBT, sc-67392). For cell culture immunostaining, primary antibodies were used at 1:200 unless stated otherwise: afadin (Sigma, A0224),  $\alpha$ -tubulin (AbD Serotec, MCA77G), Podocalyxin (DSHB, 3F2/D8), ZO1 (Millipore, MABT11), cadherin 6 (a gift of G. Dressler, University of Michigan, MI, USA), and Phalloidin 647 (Invitrogen, 42008A). For cell western blots, we used afadin (1:1000, Sigma, A0224) and  $\beta$ -actin (1:5000, Abcam, ab8227) antibodies with HRP-conjugated secondary antibodies (Jackson ImmunoResearch) at 1:5000–1:10,000.

### Measurement of the orientation of cell division

In MDCK cells, immunofluorescence was performed with antibodies to  $\alpha$ -tubulin and podocalyxin to visualize the mitotic spindle and apical surface of cysts. Cysts were imaged using a Zeiss LSM 510 META confocal laser-scanning microscope at the largest cross-sectional diameter (equatorial plane). Spindle coordinates ( $x_1, y_1$ ) and ( $x_2, y_2$ ) of a mitotic cell were used to generate vector  $V_s$ . In 5-day cysts, the midpoint ( $x_m, y_m$ ) of  $V_s$  was calculated and the center ( $x_c, y_c$ ) of each cyst was determined using an ImageJ macro. A radial vector  $V_c$  was generated from ( $x_c, y_c$ ) and ( $x_m, y_m$ ). The projected angle  $\phi$  between  $V_s$  and  $V_c$  was defined as the apical basal spindle angle, and was calculated as  $\phi = \text{acos}((V_c \cdot V_s) / (||V_c|| ||V_s||))$ . In early cysts (two cells), the reference vector was obtained from the cell-cell interface, and calculations were performed similarly.

For nephron tubules, we immunostained sections with antibodies to the basolateral marker NCAM and apical marker Par6b, and utilized a nuclear marker to label DNA. Confocal z-stacks were collected. We visualized nuclei rather than the spindle because multiple antibodies to spindle components gave insufficient signal through the depth of the z-stack. Because tubules were curved, we determined the local longitudinal vector of the tubule and performed a 3D rotation using Matlab such that this vector,  $V_L$ , lay along the x-axis. After the image was rotated, the spindle vector  $V_S$  was generated from the coordinates of the nuclei in anaphase ( $x, y, z$ ) and measured in ImageJ. Measurement of  $\theta$ , the angle between the 3D vectors  $V_L$  and  $V_S$  was determined as  $\theta = \text{acos}((V_L \cdot V_S) / (||V_L|| ||V_S||))$ . To measure the apical-basal component of the mitotic spindle angle ( $\phi$ ), we first calculated the midpoint of the spindle vector, and identified the center point of the tubule in the  $yz$  plane using ImageJ. A radial vector  $V_c$  was defined as the vector from the center to the spindle midpoint ( $x_1, y_1, z_1$ ) and vector  $V_s$  as ( $x_2, y_2, z_2$ ). We then calculated  $\phi$  as the following:

$$\phi = \text{acos}\left(\frac{V_c \cdot V_s}{||V_c|| ||V_s||}\right) = \frac{(y_1 \times y_2) + (z_1 \times z_2)}{\sqrt{y_1^2 + z_1^2} \times \sqrt{y_2^2 + z_2^2}}$$

$\theta$  and  $\phi$  were reported as the absolute of these angles in degrees between 0° and 90°. See pictorial representation of angles in Fig. 6A. For  $\Delta y$  and  $\Delta z$  approaching 0°,  $\phi$  was alternatively calculated using a radial vector from the lumen in an orthologous plane. All calculations were compared with approximations using the ImageJ angle tool to ensure their validity.

### Statistics

*In vitro* experiments were performed in triplicate and are representative of at least two similar experiments. All data shown are mean  $\pm$  s.d. Statistical significance was performed using an unpaired, two-tailed Student's *t*-test unless stated otherwise.

### Acknowledgements

We thank G. Dressler (U. Michigan) for the cadherin 6 antibody, N. Tang (NIBS, Beijing) for advice on spindle measurements, the UTSW Live Cell Imaging Center, and T. Carroll and M. Shiloh (UTSW) for reviewing the manuscript. We thank A. McMahon (USC) for *Wnt4-cre* mice.

### Competing interests

The authors declare no competing or financial interests.

### Author contributions

Conceptualization: P.R.B., K.E.M., D.M.B., D.K.M.; Methodology: L.G., Z.Y., C.H., S.E.Z., P.R.B., D.K.M.; Software: K.L.P., D.K.M.; Validation: L.G., Z.Y., C.H., D.K.M.;

Formal analysis: L.G., Z.Y., C.H., S.E.Z., D.K.M.; Investigation: L.G., Z.Y., C.H., S.E.Z., B.L., D.K.M.; Resources: K.E.M., D.K.M.; Data curation: C.H.; Writing - original draft: D.K.M.; Writing - review & editing: L.G., Z.Y., C.H., P.R.B., K.E.M., D.M.B., D.K.M.; Visualization: S.E.Z., D.K.M.; Supervision: Z.Y., D.K.M.; Project administration: S.E.Z., D.K.M.; Funding acquisition: K.E.M., D.K.M.

### Funding

This work was supported by Basil O'Connor Starter Scholar Research Award from the March of Dimes Foundation (5-FY13-201 to D.K.M.), a Satellite Healthcare Norman S. Coplon grant (to D.K.M.), the National Institutes of Health (R01DK099478 to D.K.M., R01DK074398 to K.E.M., R01DK091530 to K.E.M.) and a grant from the O'Brien Kidney Center (P30DK079328 to O. Moe, University of Texas Southwestern, TX, USA). Deposited in PMC for release after 12 months.

### Supplementary information

Supplementary information available online at <http://dev.biologists.org/lookup/doi/10.1242/dev.148908.supplemental>

### References

- Bañón-Rodríguez, I., Gálvez-Santisteban, M., Vergarajauregui, S., Bosch, M., Borreguero-Pascual, A. and Martín-Belmonte, F. (2014). EGFR controls IQGAP basolateral membrane localization and mitotic spindle orientation during epithelial morphogenesis. *EMBO J.* **33**, 129-145.
- Boettner, B., Govek, E.-E., Cross, J. and Van Aelst, L. (2000). The junctional multidomain protein AF-6 is a binding partner of the Rap1A GTPase and associates with the actin cytoskeletal regulator profilin. *Proc. Natl. Acad. Sci. USA* **97**, 9064-9069.
- Bryant, D. M., Datta, A., Rodríguez-Fraticelli, A. E., Peränen, J., Martín-Belmonte, F. and Mostov, K. E. (2010). A molecular network for de novo generation of the apical surface and lumen. *Nat. Cell Biol.* **12**, 1035-1045.
- Carmena, A., Makarova, A. and Speicher, S. (2011). The Rap1-Rgl-Ral signaling network regulates neuroblast cortical polarity and spindle orientation. *J. Cell Biol.* **195**, 553-562.
- Carminati, M., Gallini, S., Pirovano, L., Alfieri, A., Bisi, S. and Mapelli, M. (2016). Concomitant binding of Afadin to LGN and F-actin directs planar spindle orientation. *Nat. Struct. Mol. Biol.* **23**, 155-163.
- Cerruti, B., Puliafito, A., Shewan, A. M., Yu, W., Combes, A. N., Little, M. H., Chianale, F., Primo, L., Serini, G., Mostov, K. E. et al. (2013). Polarity, cell division, and out-of-equilibrium dynamics control the growth of epithelial structures. *J. Cell Biol.* **203**, 359-372.
- Cong, L. and Zhang, F. (2015). Genome engineering using CRISPR-Cas9 system. *Methods Mol. Biol.* **1239**, 197-217.
- Durgan, J., Kaji, N., Jin, D. and Hall, A. (2011). Par6B and atypical PKC regulate mitotic spindle orientation during epithelial morphogenesis. *J. Biol. Chem.* **286**, 12461-12474.
- Fischer, E., Legue, E., Doyen, A., Nato, F., Nicolas, J. F., Torres, V., Yaniv, M. and Pontoglio, M. (2006). Defective planar cell polarity in polycystic kidney disease. *Nat. Genet.* **38**, 21-23.
- Hao, Y., Du, Q., Chen, X., Zheng, Z., Balsbaugh, J. L., Maitra, S., Shabanowitz, J., Hunt, D. F. and Macara, I. G. (2010). Par3 controls epithelial spindle orientation by aPKC-mediated phosphorylation of apical Pins. *Curr. Biol.* **20**, 1809-1818.
- Iruela-Arispe, M. L. and Beitel, G. J. (2013). Tubulogenesis. *Development* **140**, 2851-2855.
- Jaffe, A. B., Kaji, N., Durgan, J. and Hall, A. (2008). Cdc42 controls spindle orientation to position the apical surface during epithelial morphogenesis. *J. Cell Biol.* **183**, 625-633.
- Karner, C. M., Chirumamilla, R., Aoki, S., Igarashi, P., Wallingford, J. B. and Carroll, T. J. (2009). Wnt9b signaling regulates planar cell polarity and kidney tubule morphogenesis. *Nat. Genet.* **41**, 793-799.
- Kim, M., Shewan, A. M., Ewald, A. J., Werb, Z. and Mostov, K. E. (2015). p114RhoGEF governs cell motility and lumen formation during tubulogenesis through a ROCK-myosin-II pathway. *J. Cell Sci.* **128**, 4317-4327.
- Klinkert, K., Rocancourt, M., Houdusse, A. and Echard, A. (2016). Rab35 GTPase couples cell division with initiation of epithelial apico-basal polarity and lumen opening. *Nat. Commun.* **7**, 11166.
- Kobayashi, A., Valerius, M. T., Mugford, J. W., Carroll, T. J., Self, M., Oliver, G. and McMahon, A. P. (2008). Six2 defines and regulates a multipotent self-renewing nephron progenitor population throughout mammalian kidney development. *Cell Stem Cell* **3**, 169-181.
- Li, D., Mangan, A., Cicchini, L., Margolis, B. and Prekeris, R. (2014). FIP5 phosphorylation during mitosis regulates apical trafficking and lumenogenesis. *EMBO Rep.* **15**, 428-437.
- Linnemann, T., Geyer, M., Jaitner, B. K., Block, C., Kalbitzer, H. R., Wittinghofer, A. and Herrmann, C. (1999). Thermodynamic and kinetic characterization of the interaction between the Ras binding domain of AF6 and members of the Ras subfamily. *J. Biol. Chem.* **274**, 13556-13562.
- Mandai, K., Rikitake, Y., Shimono, Y. and Takai, Y. (2013). Afadin/AF-6 and canoe: roles in cell adhesion and beyond. *Prog. Mol. Biol. Transl. Sci.* **116**, 433-454.
- Marciano, D. K. (2017). A holey pursuit: lumen formation in the developing kidney. *Pediatr. Nephrol.* **32**, 7-20.
- Marciano, D. K., Brakeman, P. R., Lee, C.-Z., Spivak, N., Eastburn, D. J., Bryant, D. M., Beaudoin, G. M., III, Hofmann, I., Mostov, K. E. and Reichardt, L. F. (2011). p120 catenin is required for normal renal tubulogenesis and glomerulogenesis. *Development* **138**, 2099-2109.
- Monteiro, A. C., Sumagin, R., Rankin, C. R., Leoni, G., Mina, M. J., Reiter, D. M., Stehle, T., Dermody, T. S., Schaefer, S. A., Hall, R. A. et al. (2013). JAM-A associates with ZO-2, afadin, and PDZ-GEF1 to activate Rap2c and regulate epithelial barrier function. *Mol. Biol. Cell* **24**, 2849-2860.
- Morais-De-Sá, E. and Sunkel, C. (2013). Adherens junctions determine the apical position of the midbody during follicular epithelial cell division. *EMBO Rep.* **14**, 696-703.
- Mostov, K. E. and Deitcher, D. L. (1986). Polymeric immunoglobulin receptor expressed in MDCK cells transcytoses IgA. *Cell* **46**, 613-621.
- Mugford, J. W., Yu, J., Kobayashi, A. and McMahon, A. P. (2009). High-resolution gene expression analysis of the developing mouse kidney defines novel cellular compartments within the nephron progenitor population. *Dev. Biol.* **333**, 312-323.
- Nishio, S., Tian, X., Gallagher, A. R., Yu, Z., Patel, V., Igarashi, P. and Somlo, S. (2010). Loss of oriented cell division does not initiate cyst formation. *J. Am. Soc. Nephrol.* **21**, 295-302.
- O'Brien, L. E., Jou, T.-S., Pollack, A. L., Zhang, Q., Hansen, S. H., Yurchenco, P. and Mostov, K. E. (2001). Rac1 orientates epithelial apical polarity through effects on basolateral laminin assembly. *Nat. Cell Biol.* **3**, 831-838.
- Packard, A., Georgas, K., Michos, O., Riccio, P., Cebrian, C., Combes, A. N., Ju, A., Ferrer-Vaquer, A., Hadjantonakis, A. K., Zong, H. et al. (2013). Luminal mitosis drives epithelial cell dispersal within the branching ureteric bud. *Dev. Cell* **27**, 319-330.
- Rakotomamonjy, J., Brunner, M., Juschke, C., Zang, K., Huang, E. J., Reichardt, L. F. and Chenn, A. (2017). Afadin controls cell polarization and mitotic spindle orientation in developing cortical radial glia. *Neural Dev.* **12**, 7.
- Reinsch, S. and Karsenti, E. (1994). Orientation of spindle axis and distribution of plasma membrane proteins during cell division in polarized MDCKII cells. *J. Cell Biol.* **126**, 1509-1526.
- Saburi, S., Hester, I., Fischer, E., Pontoglio, M., Eremina, V., Gessler, M., Quaggin, S. E., Harrison, R., Mount, R. and McNeill, H. (2008). Loss of Fat4 disrupts PCP signaling and oriented cell division and leads to cystic kidney disease. *Nat. Genet.* **40**, 1010-1015.
- Sato, T., Fujita, N., Yamada, A., Ooshio, T., Okamoto, R., Irie, K. and Takai, Y. (2006). Regulation of the assembly and adhesion activity of E-cadherin by nectin and afadin for the formation of adherens junctions in Madin-Darby canine kidney cells. *J. Biol. Chem.* **281**, 5288-5299.
- Sawyer, J. K., Choi, W., Jung, K.-C., He, L., Harris, N. J. and Peifer, M. (2011). A contractile actomyosin network linked to adherens junctions by Cnca/afadin helps drive convergent extension. *Mol. Biol. Cell.* **22**, 2491-2508.
- Saxen, L. (1987). *Organogenesis of the Kidney*. New York: Cambridge University Press.
- Schluter, M. A., Pfarr, C. S., Pieczynski, J., Whiteman, E. L., Hurd, T. W., Fan, S., Liu, C.-J. and Margolis, B. (2009). Trafficking of Crumbs3 during cytokinesis is crucial for lumen formation. *Mol. Biol. Cell* **20**, 4652-4663.
- Schober, M., Schaefer, M. and Knoblich, J. A. (1999). Bazooka recruits Inscuteable to orient asymmetric cell divisions in Drosophila neuroblasts. *Nature* **402**, 548-551.
- Sims-Lucas, S., Di Giovanni, V., Schaefer, C., Cusack, B., Eswarakumar, V. P. and Bates, C. M. (2012). Ureteric morphogenesis requires Fgfr1 and Fgfr2/ Frs2alpha signaling in the metanephric mesenchyme. *J. Am. Soc. Nephrol.* **23**, 607-617.
- Tang, N., Marshall, W. F., McMahon, M., Metzger, R. J. and Martin, G. R. (2011). Control of mitotic spindle angle by the RAS-regulated ERK1/2 pathway determines lung tube shape. *Science* **333**, 342-345.
- Wee, B., Johnston, C. A., Prehoda, K. E. and Doe, C. Q. (2011). Canoe binds RanGTP to promote Pins(TPR)/Mud-mediated spindle orientation. *J. Cell Biol.* **195**, 369-376.
- Wodarz, A., Ramrath, A., Kuchinke, U. and Knust, E. (1999). Bazooka provides an apical cue for Inscuteable localization in Drosophila neuroblasts. *Nature* **402**, 544-547.
- Yang, Z., Zimmerman, S., Brakeman, P. R., Beaudoin, G. M., III, Reichardt, L. F. and Marciano, D. K. (2013). De novo lumen formation and elongation in the developing nephron: a central role for afadin in apical polarity. *Development* **140**, 1774-1784.
- Yu, J., Carroll, T. J. and McMahon, A. P. (2002). Sonic hedgehog regulates proliferation and differentiation of mesenchymal cells in the mouse metanephric kidney. *Development* **129**, 5301-5312.



## Figure S1

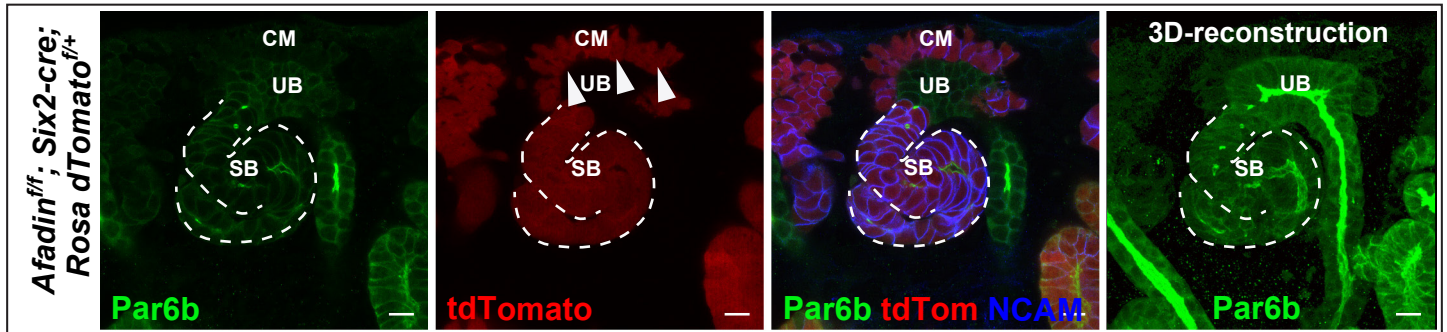


*Fig S1. The Six2-cre allele causes recombination in nephron progenitors with high efficiency.*

Immunofluorescence of tdTomato (red) in E17.5 *Afadin<sup>fl/fl</sup>; Rosa26R tdTomato<sup>fl/fl</sup>; Six2-cre* kidneys indicates *Six2-cre* induces recombination in nephron progenitors of the cap mesenchyme (CM, arrowheads) with high efficiency and specificity. The images are also immunostained with Par6b (green) to show the discontinuous lumens in the s-shaped body (SB), denoted by dotted lines. NCAM (blue) marks the lateral cell membranes on nephron tubules. A 3D reconstruction of the lumen is also shown (right).

SB, s-shaped body; CM, cap mesenchyme; UB, ureteric epithelia.

Scale bars: 10  $\mu$ m.

## Figure S2

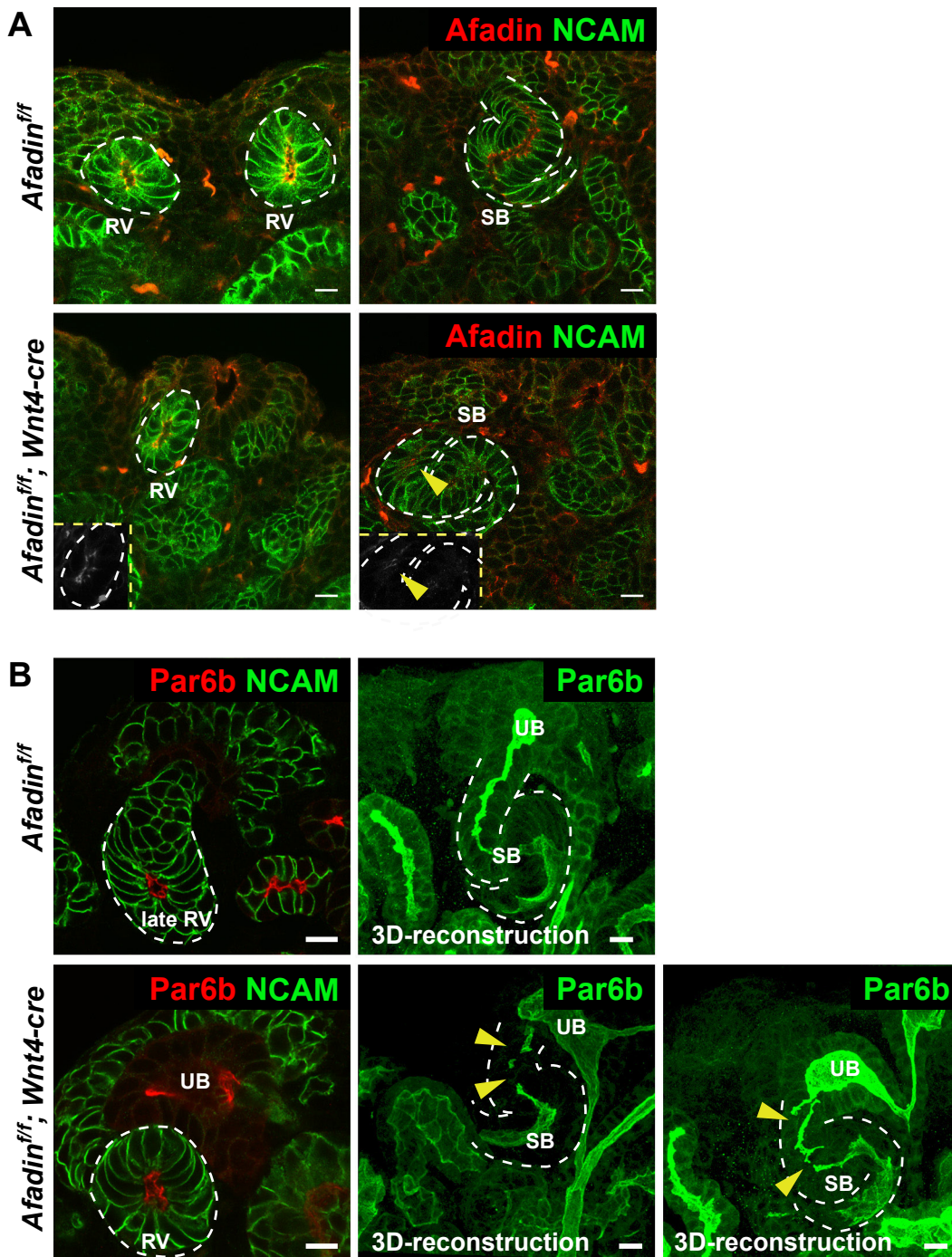


Fig S2. *Afadin*<sup>fl/fl</sup>; *Wnt4-cre* mice have discontinuous lumens in s-shaped bodies but no delay in lumen initiation

(A) Immunofluorescence with Afadin (red, white in insets) shows it is present in renal vesicles (RV) of *Afadin*<sup>fl/fl</sup>; *Wnt4-cre* kidneys at levels similar to *Afadin*<sup>fl/fl</sup> controls. Only low levels of Afadin are present in s-shaped bodies (SB) of *Afadin*<sup>fl/fl</sup>; *Wnt4-cre* kidneys compared to controls. Afadin in the s-shaped body of an *Afadin*<sup>fl/fl</sup>; *Wnt4-cre* kidney is indicated by yellow arrowheads.

(B) *Afadin*<sup>fl/fl</sup>; *Wnt4-cre* kidneys have normal appearing lumens in renal vesicles, but discontinuous lumens in s-shaped bodies. Immunofluorescence with Par6b, which marks the apical surface, shows control and mutant renal vesicles have central lumens (left panels). NCAM marks the lateral cell membranes on nephron progenitors and renal vesicles. In the right panels, 3D reconstructions of z-stacks show s-shaped body lumens are continuous in controls, but not mutants. Discontinuities are indicated by yellow arrowheads. The ureteric epithelia (UB) is indicated. Scale bars: 10 μm.

## Figure S3

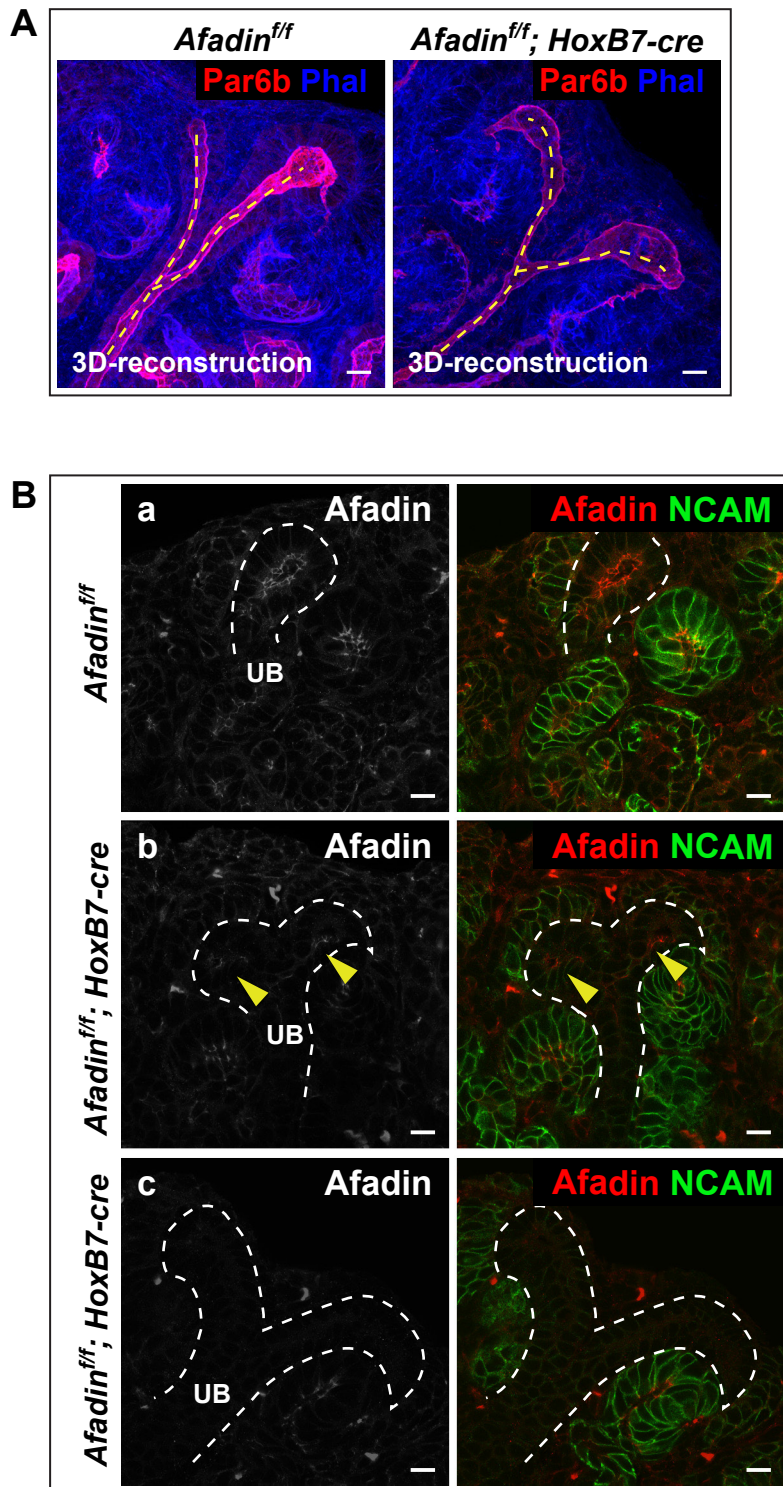
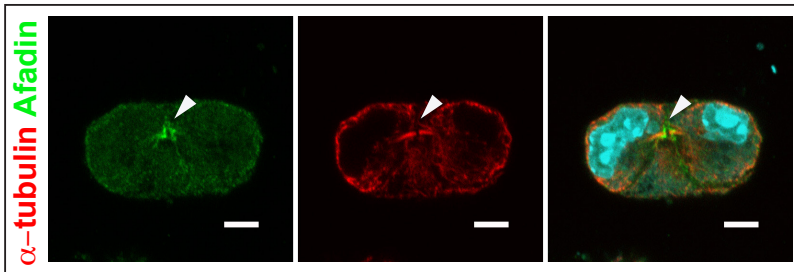


Fig S3. *Afadin<sup>fl/fl</sup>; HoxB7-cre* mice have continuous lumens in ureteric epithelial tubules, but many have residual *afadin*. (A) 3D reconstructions of z-stacks from kidneys immunostained with Par6b, which marks the apical/luminal surface (red), shows control (*Afadin<sup>fl/fl</sup>*) and mutant (*Afadin<sup>fl/fl</sup>; HoxB7-cre*) ureteric tubules have continuous lumens. The ureteric lumens are highlighted with yellow dotted lines. F-actin is stained with phalloidin (Phal, blue). (B) Immunofluorescence with Afadin shows it is present in ureteric epithelia of *Afadin<sup>fl/fl</sup>* mice, but reduced (Ba) or absent (Bc) in *Afadin<sup>fl/fl</sup>; HoxB7-cre* mice. Yellow arrowheads indicate residual *afadin* in *Afadin<sup>fl/fl</sup>; HoxB7-cre* ureteric epithelia in Bb. Scale bars: 10  $\mu$ m.



## Figure S4



### *Fig S1. Afadin localizes to the midbody*

Immunofluorescence of  $\alpha$ -tubulin (red) and Afadin (green) shows the localization of the midbody (arrowhead), which is enriched in microtubules, in an early MDCK cell cyst.

Scale bars: 5  $\mu$ m.

Table S1. Afadin shRNAs and sgRNAs utilized in this paper.

shRNA/sgRNA	Primer names	Primer sequences
Afadin shRNA	shRNA-AF-1 (F)	5'- CCGG <b>GACAATCCTGCTGTCTACC</b> CTCGAG <b>GGTAGACAGCAGGATTGTC</b> TTTTGTG -3'
	shRNA-AF-1 (R)	5'- AATTCAAAAA <b>GACAATCCTGCTGTCTACC</b> CTCGAG <b>GGTAGACAGCAGGATTGTC</b> -3'
Afadin sgRNA exon 2	sgRNA-AF-1 (F)	5'- CACCg <b>TGGAATAAAGATGATCGAGA</b> -3'
	sgRNA-AF-1 (R)	5'- AAAC <b>TCTCGATCATCTTTATTCCA</b> c -3'
Afadin sgRNA exon 3	sgRNA-AF-3 (F)	5'- CACCg <b>CCTTCTTTCTCCTGCTTTTC</b> -3'
	sgRNA-AF-3 (R)	5'- AAAC <b>GAAAAGCAGGAGAAAGAAGG</b> c -3'